

Dab2, Megalin, Cubilin and Amnionless Receptor Complex Might Mediate Intestinal Endocytosis in the Suckling Rat

María D. Vázquez-Carretero,¹ Marta Palomo,¹ Pablo García-Miranda,¹ Inmaculada Sánchez-Aguayo,² María J. Peral,¹ María L. Calonge,^{1*} and Anunciación A. Ilundain¹

¹Departamento de Fisiología, Facultad de Farmacia, Universidad de Sevilla, Spain

²Departamento de Biología Celular, Facultad de Biología, Universidad de Sevilla, Spain

ABSTRACT

We previously proposed that Dab2 participates in the endocytosis of milk macromolecules in rat small intestine. Here we investigate the receptors that may mediate this endocytosis by studying the effects of age and diet on megalin, VLDLR, and ApoER2 expression, and that of age on the expression of cubilin and amnionless. Of megalin, VLDLR and ApoER2, only the megalin expression pattern resembles that of Dab2 previously reported. Thus the mRNA and protein levels of megalin and Dab2 are high in the intestine of the suckling rat, down-regulated by age and up-regulated by milk diet, mainly in the ileum. Neither age nor diet affect ApoER2 mRNA levels. The effect of age on VLDLR mRNA levels depends on the epithelial cell tested but they are down-regulated by milk diet. In the suckling rat, the intestinal expressions of both cubilin and amnionless are similar to that of megalin and megalin, cubilin, amnionless and Dab2 co-localize at the microvilli and in the apical endocytic apparatus. Co-localization of Dab2 with ApoER2 and VLDLR at the microvilli and in the apical endocytic apparatus is also observed. This is the first report showing intestinal co-localization of: megalin/cubilin/amnionless/Dab2, VLDLR/Dab2 and ApoER2/Dab2. We conclude that the megalin/cubilin/amnionless/Dab2 complex/es participate in intestinal processes, mainly during the lactation period and that Dab2 may act as an adaptor in intestinal processes mediated by ApoER2 and VLDLR. *J. Cell. Biochem.* 115: 510–522, 2014. © 2013 Wiley Periodicals, Inc.

KEY WORDS: Dab2; MEGALIN; CUBILIN; AMNIONLESS; INTESTINE

In the suckling mammals, the epithelium of the small intestine has a highly endocytic activity which enables the enterocytes the absorption of the macromolecules present in maternal colostrum and milk, such as growth factors and immunoglobulins. To achieve this, the enterocytes of the suckling animal have an apical endocytic complex comprised of an elaborate array of membrane tubules and vesicles beneath the microvillus membrane [Fujita et al., 2007]. At weaning the diet gradually changes from a maternal milk diet to solid nutrition and the gut undergoes dramatic structural and functional changes before adult patterns are developed. During this period the suckling absorptive cells of the jejunum and ileum are completely replaced by adult absorptive cells and their apical endocytic membrane system is greatly reduced [Fujita et al., 2007]. Consequently the epithelial permeability to macromolecules abruptly stops after weaning [Fujita et al., 2007] and the adult enterocytes are mainly

confined to small molecule absorption. However, endocytosis plays a key role in cell homeostasis and signaling through life. Via endocytosis cells internalize plasma membrane components, control the composition of the plasma membrane, the signaling receptors and the recycling of transmembrane proteins [Keita and Söderholm, 2010].

Endocytosis mediated by clathrin-coated vesicles is considered the most important pathway for internalization of macromolecules during intestinal development [Keita and Söderholm, 2010] and is highly active during the suckling period [see Fujita et al., 2007 for a review]. The clathrin-mediated endocytosis requires the action of endocytic adaptor proteins to organize clathrin assembly and recruit cargo, other adaptor proteins and transmembrane receptors. There are two major classes of endocytic adaptors involved in assembly of clathrin-coated vesicles: multimeric adaptor proteins (AP2) and

Grant sponsor: Junta de Andalucía; Grant number: CTS 5884.

*Correspondence to: María L. Calonge, Departamento de Fisiología, Facultad de Farmacia, C/Profesor García González, no 2, 41012 Sevilla, Spain. E-mail: calonge@us.es

Manuscript Received: 10 April 2013; Manuscript Accepted: 26 September 2013

Accepted manuscript online in Wiley Online Library (wileyonlinelibrary.com): 5 October 2013

DOI 10.1002/jcb.24685 • © 2013 Wiley Periodicals, Inc.

monomeric adaptor proteins such as Dab2 [Maldonado-Báez and Wendland, 2006].

Dab2 binds to the cytosolic FXNPXY domain of members of the low density lipoprotein receptor (LDLR) family via its N-terminal domain [Oleinikov et al., 2000; Morris and Cooper, 2001]; to the motor protein myosin VI, implicated in endocytosis, via the C-terminal domain [Morris et al., 2002a] and to clathrin and to α -AP-2, via two motifs of its central region [Morris and Cooper, 2001; Mishra et al., 2002; Cihil et al., 2012]. All these interactions endow Dab2 the role of coordinating vesicle coat assembly, cargo recruitment, vesicle formation and vesicle traffic.

The role of Dab2 in endocytosis was first discovered in the epithelium of rat renal proximal tubule [Morris et al., 2002b; Nagai et al., 2005] and mouse visceral endoderm [Maurer and Cooper, 2005]. In these tissues Dab2 acts as an adaptor protein in the megalin-mediated endocytosis of filtered proteins and of transferrin, respectively. Megalin (600 kDa) belongs to the LDLR family and other members of this family are apolipoprotein E receptor 2 (ApoER2) and the very low-density lipoprotein receptor (VLDLR). Two reports previously have linked these two receptors with Dab2. Cuitino et al. [2005] found that Dab2 interacts with ApoER2 in culture cells and participates in its endocytosis and Yang et al. [2002] reported that Dab2 does not bind to VLDLR. Dab2 also interacts with amnionless [Pedersen et al., 2010], a transmembrane protein of 50 kDa that has two FXNPXF cytosolic signals that resemble the FXNPXY signal of the LDLR family. Amnionless binds tightly with cubilin (460 kDa) and forms the cubilin/amnionless receptor complex [Fyfe et al., 2004]. Cubilin is a multiligand receptor that has neither a transmembrane segment nor the classical signals for endocytosis [Moestrup et al., 1998] and amnionless is required to drive and anchor cubilin to the cell membrane [Fyfe et al., 2004; He et al., 2005]. Cubilin also forms an oligomeric complex with megalin in the kidney (see Seetharam and Yammani, 2003 for a review) and megalin drives endocytosis of cubilin and its ligands in kidney [Moestrup et al., 1998; Christensen and Verroust, 2002; Amsellem et al., 2010] and yolk sac [Hammad et al., 2000]. Association of cubilin with megalin has also been observed in rat small intestine [Yammani et al., 2001], but in the intestine amnionless appears to facilitate the internalization of cubilin in megalin-deficient patients [Christensen et al., 2013]. More recently, Ahuja et al. [2008] reported that in renal apical membrane vesicles megalin/cubilin/amnionless complex exists as a functional endocytic receptor.

Dab2 has also been implicated in non-receptor mediated endocytosis. In the intestine Dab2 acts as an adaptor protein in the apical endocytosis of the cystic fibrosis transmembrane conductance regulator (CFTR) chloride channel. However, CFTR does not contain a recognized Dab2 binding motif and here Dab2 interacts with α -AP2 [Collaco et al., 2010].

We previously reported that the expression of Dab2 in rat enterocytes is down-regulated by ontogeny and up-regulated by milk diet. Based on these observations we suggested that Dab2 is involved in the apical endocytosis of milk macromolecules [Vázquez-Carretero et al., 2011], but nothing is known on the endocytic receptors that interact with Dab2 in the small intestine. Megalin [Birn et al., 1997; Yammani et al., 2001], cubilin [Birn et al., 1997], ApoER2 [García-Miranda et al., 2010] and VLDLR [García-Miranda et al., 2010] have

been localized at the apical membrane of the small intestinal epithelium. The purpose of the present series of experiments was to investigate whether these receptors and Dab2 are involved in the endocytosis of milk components.

A preliminary report of some of these results was published as an abstract [Vázquez-Carretero et al., 2012].

MATERIAL AND METHODS

CHEMICALS

The antibodies: rabbit anti-Dab2 (sc-13982), mouse anti-VLDLR (sc-18824), rabbit anti-cubilin (sc-50319) and rabbit anti-megalin (sc-16478) were obtained from Santa Cruz Biotechnology, Inc., Dallas, TX; mouse anti-Dab2 (610464) from BD Transduction Laboratories; mouse anti-megalin (DM3613) from Acris; mouse anti-ApoER2 (ab58216) from AbCam; sheep anti-Amnionless (AF7139) from R&D Systems and anti- β -actin from Sigma-Aldrich, Madrid, Spain. Biotin-conjugated anti-sheep IgG, anti-rabbit IgG, anti-mouse IgG and anti-goat IgG were obtained from Vector Laboratories. Gold-conjugated anti-mouse IgG (10 nm gold), anti-rabbit IgG (6 nm gold) and anti-sheep IgG (15 nm gold) secondary antibodies were obtained from Aurion. All antibodies are immune affinity purified and immune cross-adsorbed by the manufacturers to diminish, and frequently prevent, non-specific reactions. Unless otherwise indicated, the reagents used in this study were from Sigma-Aldrich.

ANIMALS AND DIETS

Suckling (5 and 12–15 day-postpartum), weaning (21 day-postpartum) and adult (30 day-old) Wistar rats were used. Adult rats were fed with a rat diet (Harlan Ibérica S.L., Barcelona, Spain) *ad libitum* and had free access to tap water. For some experiments, 15 day-old rats were weaned onto either rat chow or dry commercial milk like mother's (Cyntech Health Nutrition) and maintained under these experimental conditions up to either day 21 or 30.

The animals were humanely handled and sacrificed with a lethal intraperitoneal injection of pentobarbital (50 mg/kg), in accordance with the European Council legislation 86/609/EEC concerning the protection of experimental animals.

ISOLATION OF ENTEROCYTES AND CRYPTS

The jejunum and ileum were rapidly removed and washed with ice-cold saline solution. Enterocytes and crypts were sequentially isolated by a Ca^{2+} -chelation technique [Weiser, 1973] as modified by Knickelbein et al. [1988]. Briefly, 2 cm intestinal segments were incubated in a shaking water bath at 37°C for 15 min. The incubation buffer contained in mM: 96 NaCl, 27 $\text{Na}_3\text{C}_3\text{H}_5\text{O}(\text{COO})_3$, 0.8 KH_2PO_4 , 5.6 Na_2HPO_4 , 1.5 KCl, 10 glucose and 0.5 dithiothreitol, pH 7.4 (buffer A) and it was continuously gassed with 95% O_2 –5% CO_2 . Following incubation, the intestinal pieces were incubated for 20 min at 37°C in PBS (in mM: 137 NaCl, 2.7 KCl, 10.1 Na_2HPO_4 and 1.8 KH_2PO_4 , pH 7.4) containing, in mM: 1.5 EDTA, 10 glucose and 0.5 dithiothreitol (buffer B). The tissues were vortexed for 30 s to remove epithelial cells from the villi. Loosened epithelial cells were filtered through 60 μm nylon cloth and collected by centrifugation and resuspension in PBS. They constitute the enterocytes enriched fraction. The tissues were incubated for another 10 min in buffer B and the buffer discarded.

Following a 20 min incubation period in buffer B, the tissues were vortexed for 5 min and the crypt cells collected by centrifugation and resuspension in PBS. The isolated cells were used immediately for immunostaining or frozen in liquid nitrogen and kept at -80°C until used for RNA extraction. The cell enrichment of each fraction was evaluated by measuring the mRNA abundance of markers characteristic of enterocytes, SGLT1 [Hwang et al., 1991], and of crypt cells, $\text{Na}^{+}\text{-K}^{+}\text{-2Cl}^{-}$ cotransporter 1 (NKCC1) [Matthews et al., 1998]. The enrichment factor is defined as the ratio of the mRNA levels in the two compartments. The SGLT1 mRNA abundance in the enterocytes fraction versus that measured in the crypts fraction is 7 ± 0.5 fold in the jejunum and 6.3 ± 0.4 fold in the ileum ($n = 4$). Reciprocally, the NKCC1 mRNA abundance in the crypts fraction versus that in the enterocytes fraction is 7 ± 0.3 in the jejunum and 6.2 ± 0.6 in the ileum ($n = 4$). These data indicate an enrichment factor in each fraction of ~ 6.5 .

RELATIVE QUANTIFICATION OF REAL-TIME PCR

Total RNA was extracted from the enterocytes and crypts enriched fractions, obtained from the jejunum and ileum of rats of different ages, using RNeasy[®] kit (Qiagen, Germantown, MD). Sample purity was assessed by measuring $\text{OD}_{260/280}$ by spectrophotometry. RNA integrity was analyzed by visual inspection after electrophoresis on an agarose gel in the presence of ethidium bromide. cDNA was synthesized from $1 \mu\text{g}$ of total RNA using QuantiTect[®] reverse transcription kit (Qiagen) as described by the manufacturer. The primers for megalin, ApoER2, VLDLR, amnionless and cubilin were chosen according to the rat cDNA sequences entered in Genbank and designed using PerlPrimer program v1.1.14 (Parkville, Melbourne, Victoria, Australia; see Table SI). Real-time PCR was performed with iQ[™]SYBR[®] Green Supermix (BioRad, Hercules, CA), $0.4 \mu\text{M}$ primers and $1 \mu\text{l}$ cDNA. Controls were carried out without cDNA. Amplification was run in a MiniOpticon[™] System (BioRad) thermal cycler ($94^{\circ}\text{C}/3 \text{ min}$; 35 cycles of $94^{\circ}\text{C}/40$, $58^{\circ}\text{C}/40$, and $72^{\circ}\text{C}/40 \text{ s}$, and $72^{\circ}\text{C}/2 \text{ min}$). Following amplification, a melting curve analysis was performed by heating the reactions from 65 to 95°C in 1°C intervals while monitoring fluorescence. Analysis confirmed a single PCR product at the predicted melting temperature. The PCR primers efficiencies ranged from 90% to 110%. The cycle at which each sample crossed a fluorescence threshold, Ct, was determined, and the triplicate values for each cDNA were averaged. Analyses of real-time PCR were done using the comparative Ct method, with the Gene Expression Macro software supplied by BioRad. β -actin served as reference gene and was used for samples normalization. The $2^{-\Delta\text{Ct}}$ method was used to validate β -actin as internal control gene [Livak and Schmittgen, 2001].

IMMUNOBLOTTING

Dot blot assay was used to identify and quantify megalin in the apical membranes of the intestinal epithelium. Apical membranes were obtained from the jejunum and ileum by Mg^{2+} precipitation method as described [Vázquez-Carretero et al., 2011]. Briefly, the small intestine was homogenized in a buffer (in mM: 100 mannitol, 5 EGTA, 15 Tris-HCl, pH 7) with the Ystral Polytron on setting five for 1 min. MgCl_2 was added to the homogenate up to a final concentration of 10 mM. The suspension was gently stirred for 20 min and then centrifuged at

1,000 g for 15 min. The resultant supernatant was centrifuged at 30,000 g for 30 min and the resultant pellet was used for the Dot blot assays. All the steps were carried out at 4°C . Protein was measured by the method of Bradford [1976], using gamma globulin as the standard. $2 \mu\text{l}$ samples ($0.5 \mu\text{g}$ protein) were pipetted onto strips of polyvinylidene fluoride (PVDF) membrane and the membranes were left to dry for 15 min. Membranes were blocked with 5% bovine serum albumin (BSA)/Tris-buffer saline-Tween (TBS-T) for 90 min and incubated for 1 h at room temperature with anti-megalin antibody (Acris) 1:1,000 dilution in 0.1% BSA/TBS-T. The membranes were washed with TBS-T ($4 \times 10 \text{ min}$). Immunoreactivity was detected using an anti-mouse secondary antibody (1:30,000 dilution in 0.1% BSA/TBS-T) conjugated with Horseradish peroxidase. The membranes were washed again with TBS-T ($4 \times 10 \text{ min}$). Immunoreactive signals were visualised by chemiluminescence using an ECL Western Blotting Analysis System (GE Healthcare, Barcelona, Spain). Each immunoblot was performed in duplicate. Relative protein level was quantified by densitometry using the ImageJ software. The intensity corresponding to the secondary antibody alone was subtracted. Anti- β -actin antibody (1:6,000 dilution) was used to normalize density dots.

IMMUNOSTAINING ASSAYS

Immunostaining assays were performed on intact small intestine ($10 \mu\text{m}$ cryosections) and on isolated intestinal cells, as previously [García-Miranda et al., 2010]. Briefly, the small intestine was rapidly removed from the rats and washed with ice-cold saline solution. The tissue was fixed by incubation with PBS containing 4% paraformaldehyde at 4°C , overnight and cryoprotected by incubation at 4°C with 20% sucrose for 12 h and for another 12 h with 30% sucrose. $10 \mu\text{m}$ cryosections were mounted on adhesive-coated glass slides and incubated with 100% ethanol for 10 min at -20°C . Enterocytes were isolated as described above and loaded onto adhesive-coated glass slides. The cells were left to dry for 10 min at room temperature and then fixed with 2% paraformaldehyde in PBS for 30 min. The slides containing either the intestinal sections or the isolated enterocytes were washed with PBS and permeabilized with 0.1% Triton X-100 for either 10 min (tissue sections) or 20 min (isolated cells) and washed again. The slides were incubated either with anti-megalin (1:25 tissue sections, 1:250 isolated cells), anti-cubilin (1:50) or anti-amnionless (1:25) antibody, at 4°C , overnight. Controls were carried out without primary antibody. Antibody binding was visualized with biotinylated secondary antibodies, followed by immunoperoxidase staining using the Vectastain ABC peroxidase kit (Vector) and 3,3'-diaminobenzidine. The slides were mounted and photographed with a Zeiss Axioskop 40 microscope equipped with a SPOT Insight V 3.5 digital camera.

IMMUNOGOLD ELECTRON MICROSCOPY

Segments of ileum were fixed in 1% glutaraldehyde, 4% formaldehyde and 0.25% picric acid in 0.1 M phosphate buffer, pH 7.4, at room temperature for 3 h. After rinsing in phosphate buffer containing 3.5% sucrose (buffered sucrose), the segments were incubated for 1 h in 0.5 M ammonium chloride in buffered sucrose. Fixed tissue was dehydrated directly into 70% ethanol and embedded in LR White resin at 50°C for 24 h using gelatine capsules. Ultrathin sections (100 nm) were mounted on nickel grids, transferred onto PBS, blocked with 0.5% BSA diluted in PBS for 15 min and incubated with the indicated

primary antibody for 2 h at room temperature. The grids were rinsed, incubated for 1 h at room temperature with the appropriate gold-conjugated secondary antibody and washed with PBS-BSA (3 × 10 min), PBS (3 × 10 min) and distilled water (3 × 10 min). Grids were stained with 2% uranyl acetate for 10 min and washed with distilled water. Controls were carried out without primary antibody. The sections were examined under a Philips CM-10 transmission electron microscope equipped with an Olympus Veleta camera.

The microphotographs were processed with ImageJ software version 1.46 (National Institutes for Health <http://rsb.info.nih.gov/ij/index.html>) for a quantitative analysis of the distances between the immunogold particles that mark the proteins under study, following the method of Bergersen et al. [2012]. Sections were analyzed at a magnification of 64,000. A gold particle was ascribed to a morphologically identified compartment (microvilli, endocytic pits, and apical vesicles) when the centre of the particle was located within a 30 nm distance from the compartment limiting membrane. For colocalization of proteins, the intercenter distances between gold particles were measured and the distances were sorted into bins of either 20 or 40 nm. Proteins are considered to be colocalized when the intercenter distances between the gold particles is <90 nm. The frequency distributions of gold particles distances were evaluated by the Chi-squared test. For each gold particles combination, we quantified 20–30 of either microvilli, endocytic pits, or apical vesicles.

STATISTICS

Data are presented as mean ± SEM. In the figures, the vertical bars that represent the SEM are absent when they are less than symbol height. In Figure 3B comparisons between different experimental groups were evaluated by the two-tailed Student's *t*-test. One-way ANOVA followed by Newman-Keuls' test was used for multiple comparisons (GraphPad Prism program). Differences were set to be significant for $P < 0.05$. For quantitative immunogold analysis (Figs. 6–8) Chi-squared test was used. Differences were set to be significant for $P < 0.01$.

RESULTS

EFFECT OF AGE AND DIET ON INTESTINAL ApoER2, VLDLR AND MEGALIN mRNA LEVELS

ApoER2, VLDLR, and megalin mRNA levels are measured in enterocytes and crypts enriched fractions obtained from the jejunum and ileum of rats of different ages. To determine whether diet affects the expression of these receptors, rats were prevented from normal weaning by being maintained on dried milk diet, as described in Methods section. mRNA abundance was examined by Real-time PCR assay using total RNA and β -actin as internal reference gene. The use of β -actin as internal control gene has been validated with the $2^{-\Delta C_T}$ method and the results in Figure 1 show that the experimental conditions used do not significantly affect the β -actin mRNA levels.

The results summarized in Figure 2 reveal that ontogeny and diet affect the genes under study differently. ApoER2 mRNA levels are similar in jejunum and in ileum, and they are not significantly affected either by age or diet.

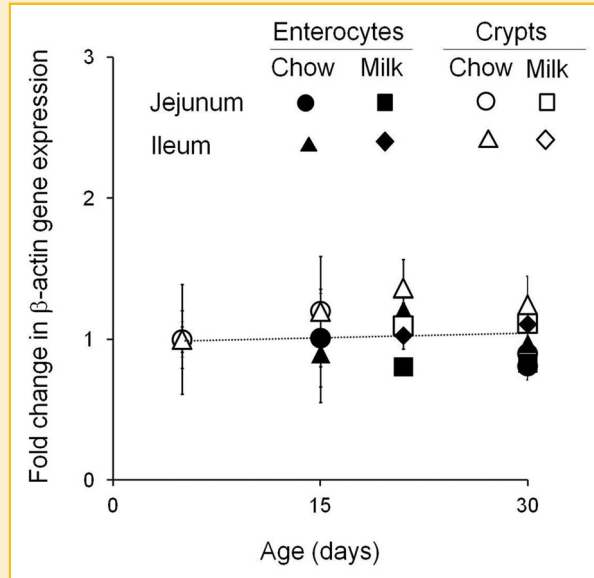


Fig. 1. Effects of epithelium cell-type, intestinal region, age and diet on relative abundance of β -actin expression. Validation of β -actin as reference gene for the RT-PCR assays was verified by the $2^{-\Delta C_T}$ method. Data are means ± SEM of four independent experiments. One-way ANOVA showed no effect of the experimental conditions used on β -actin mRNA levels.

The effects of age and diet on the VLDLR mRNA levels depend on the intestinal cell fraction examined. VLDLR mRNA levels significantly: (i) increase in the enterocytes either at weaning (jejunum) or during the suckling period (ileum), (ii) decrease in the jejunal crypts at weaning and (iii) remain more or less the same in the crypts from the ileum. Weaning the pups onto a commercial milk diet inhibits significantly VLDLR mRNA abundance in the jejunal crypts. VLDLR mRNA levels in the other intestinal cell fractions examined are not significantly affected by diet.

Megalyn mRNA levels changed with ontogeny and were affected by diet. Thus in both, enterocytes and crypts the megalyn mRNA levels: (i) measured at day 5 after birth are 20 ± 3 times higher in the ileum than in the jejunum; (ii) significantly decrease during the suckling and weaning periods, reaching adult values by day 21 after birth; the decreases are greater in the ileum than in the jejunum, and (iii) are significantly higher in the cells isolated from the ileum of pups maintained on a commercial milk diet than in those weaned onto rat chow. The milk diet does not significantly modify megalyn mRNA levels in the jejunum. No intestinal regional differences in megalyn mRNA levels were observed in 30 day-old rats.

EFFECT OF AGE AND DIET ON INTESTINAL LEVELS OF MEGALIN PROTEIN

We previously reported that Dab2 mRNA levels are higher in the ileum than in the jejunum, decrease at weaning and are up regulated by diet [Vázquez-Carretero et al., 2011]. Of the three receptors under study, only megalin mRNA expression profile resembles that of Dab2. Because of this, the effect of age and diet on protein abundance was only evaluated for megalin. This was done by the "dot blot" method

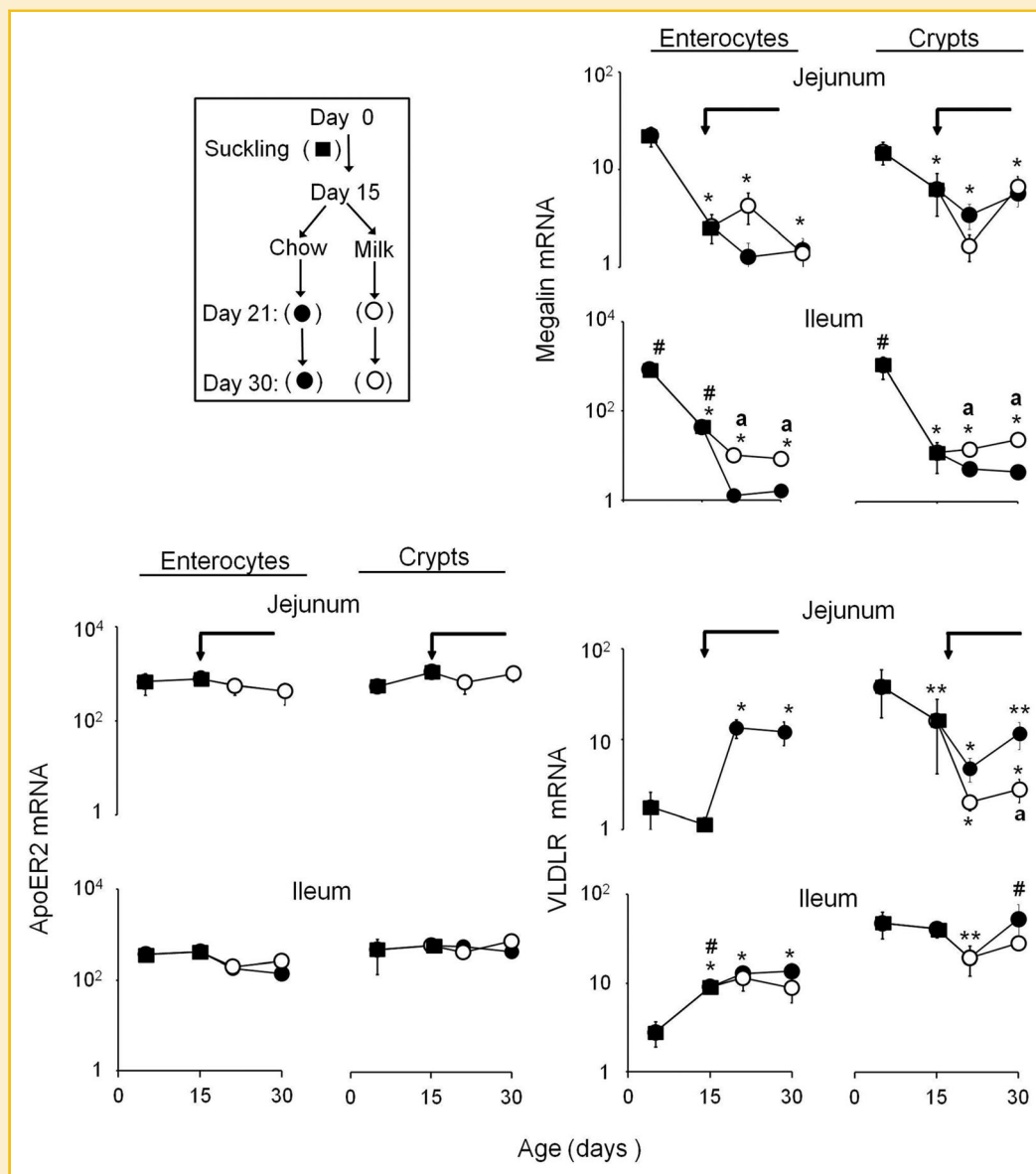


Fig. 2. Megalin, VLDLR and ApoER2 mRNA levels in rat small intestine versus age and diet. 15 day-old pups were weaned onto either rat chow (●) or commercial milk diet (○) as shown in the inset and indicated by the arrows. Enterocytes- and crypts-enriched fractions were obtained from jejunum and ileum of 5, 15, 21, and 30 day-old rats. RT-PCR was performed on total RNA obtained from each intestinal cell fraction. The VLDLR mRNA levels measured in enterocytes of 15 day-old jejunum were set at 1. Data are means \pm SEM of four independent experiments. One-way ANOVA showed an effect of maturation and intestinal region on VLDLR and Megalin mRNA levels ($P < 0.001$) and of diet on megalin mRNA levels in ileum and VLDLR mRNA levels in the jejunal crypts ($P < 0.001$). Newman-Keul's test: * $P < 0.001$; ** $P < 0.01$ as compared with 5 day-old rats, ^a $P < 0.001$ comparisons between commercial milk and rat chow; # $P < 0.001$ ileum versus jejunum.

using protein extracts from the apical membranes of enterocytes isolated from the jejunum and ileum of 5 and 30 day-old rats. The 30 days-old rats were weaned as described in Figure 2. The results (Fig. 3) reveal that megalin abundance is higher in the ileum than in the jejunum and decreases with age in both jejunum and ileum. The maintenance of the pups on a milk diet attenuated the age-related decrease in the ileum but not in the jejunum.

Together the observations presented so far suggest that intestinal expression of megalin is down-regulated by age and up-regulated by milk components.

mRNA LEVELS OF MEGALIN, CUBILIN AND AMNIONLESS IN RAT SMALL INTESTINE

The mRNA levels of the three genes were measured in enterocytes and crypts enriched fractions isolated from jejunum and ileum of 5 and 30 day-old rats. The data shown in Figure 4 reveal a similar pattern of expression for the three genes at day 5 after birth: their mRNAs levels are higher in ileum than in jejunum and of the same magnitude in enterocytes and crypts. An exception is cubilin: its mRNA levels are higher in the enterocytes than in the crypts from the jejunum.

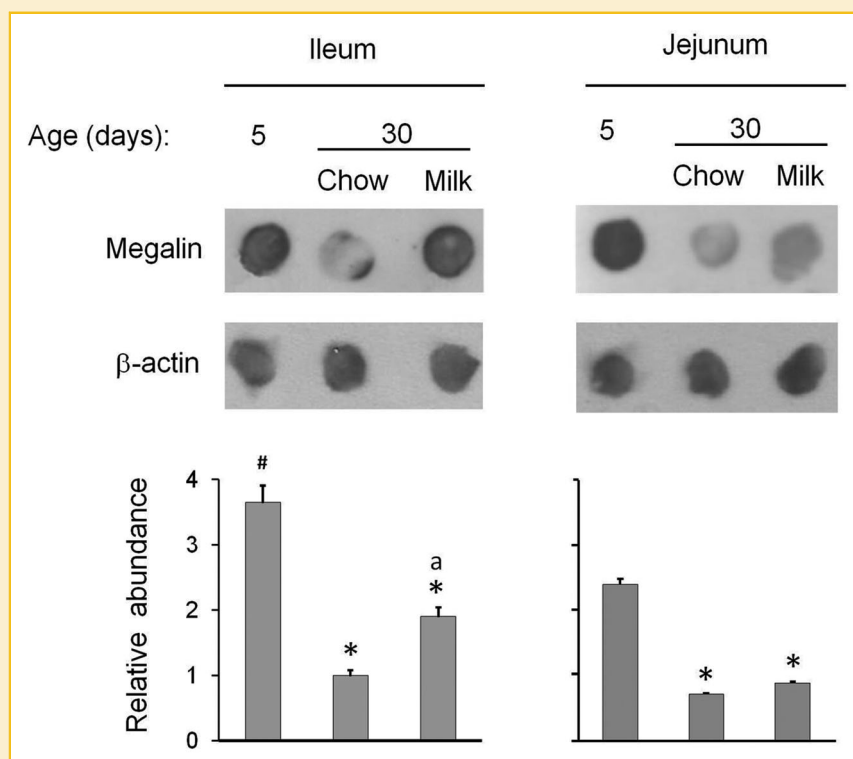


Fig. 3. Megalin protein levels in rat small intestine *versus* age and diet. Protein abundance was measured using the dot blot method. Jejunum and ileum of 5 and 30 day-old rats were used. 0.5 μ g protein extracted from enterocytes apical membrane were spotted onto PVDF membranes. Rats were weaned as described in Figure 2. Anti-megalin antibody (Acris) 1:1,000 dilution was used. Anti- β -actin antibody (1:6,000 dilution) was used to normalize the dots. Histograms represent the relative abundance of megalin protein in the apical membrane. Means \pm SEM. The blot is representative of three assays. Student's *t*-test: **P* < 0.001 as compared with 5 day-old; ^a*P* < 0.001 commercial milk *versus* chow diet; #*P* < 0.01 ileum *versus* jejunum.

However, the pattern of expression of the three genes differs at day 30 after birth. Comparing the values measured at day 30 with those measured at day 5 it is found that megalin mRNA levels are much lower, those of amnionless slightly decrease, whereas those of cubilin increase.

IMMUNOLocalIZATION OF MEGALIN, CUBILIN, AMNIONLESS AND Dab2 IN RAT SMALL INTESTINE

Megalin, cubilin, and amnionless were first immunolocalized at the light microscopy in intestine sections and in enterocytes isolated from the jejunum and ileum of 5 and 30 day-old rats. In the intestine, the specific signal produced by the three antibodies is seen in the epithelial cells lining the villi but it is absent from the crypts (Fig. 5A). In the absence of the primary antibodies labeling is absent from the tissue.

Figure 5B reveals that in the enterocytes isolated from 5 day-old rats the specific staining of the three proteins is concentrated in a cytosolic supranuclear region. At day 30, however, the immunological staining of the three proteins is mainly located at the microvilli and terminal web domain. In the absence of the primary antibodies labeling is absent from the enterocytes.

CO-LOCALIZATION OF MEGALIN, CUBILIN, AMNIONLESS AND Dab2 IN RAT SMALL INTESTINE

The subcellular distribution and co-localization of megalin, cubilin, amnionless, and Dab2 was further examined by double or triple

immunogold electron microscopy analysis. The ileum of suckling rats (12–15 days-postpartum) was chosen for these experiments because the effects of both, age and diet on the gene expression were greater in the ileum than in the jejunum. Figures 6 and 7 reveal that the immunogold particles signaling Dab2, megalin, cubilin, and amnionless are within a 30 nm distance from the limiting membrane of the microvilli, the endocytic pits, and apical vesicles, indicating that the proteins under study are located in those compartments. Figure 6 shows that the majority of intercenter distances between gold particles marking either megalin and cubilin; megalin and amnionless; cubilin and amnionless, or megalin, cubilin and amnionless are between 20 and 60 nm, indicating co-localization of these proteins at the microvilli and apical endocytic compartments. Figure 7 reveals that the distances between the gold particles signalling Dab2 and those signalling either megalin; megalin and amnionless, or cubilin and amnionless ranged from 20 to 60 nm. These observations indicates that Dab2 co-localizes at the microvilli and in the same endocytic compartments either with megalin, with megalin and amnionless or with cubilin and amnionless. Immunoreactive signal was not seen in the absence of the primary antibody (data not shown).

CO-LOCALIZATION OF VLDLR, ApoER2 AND Dab2 IN RAT SMALL INTESTINE

The ileum of suckling rats (12–15 day-postpartum) was used. Double immunogold electron microscopy analysis revealed that Dab2

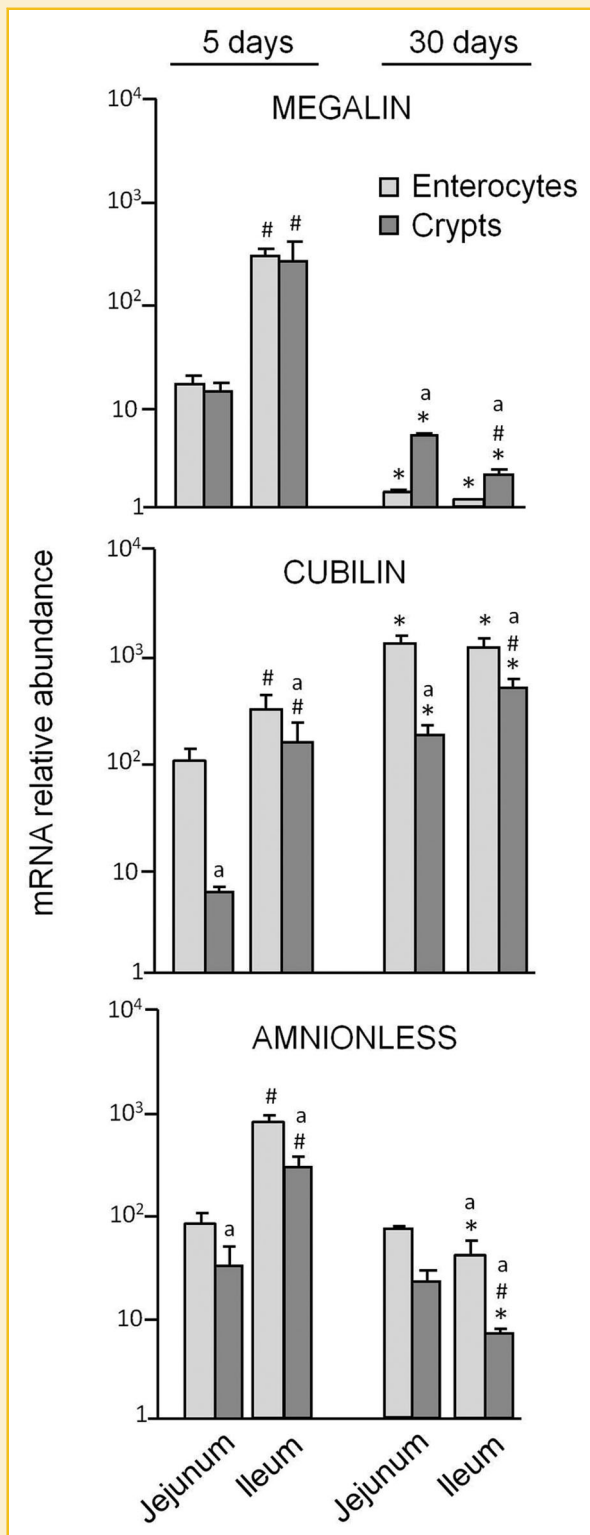


Fig. 4. Megalin, cubilin and amnionless mRNA levels in rat small intestine. 5 and 30 day-old rats were used. The megalin mRNA levels measured in the enterocytes of 30 day-old ileum were set at 1. Other details as in Figure 2. One-way ANOVA showed an effect of maturation and segmental distribution on megalin, cubilin and amnionless mRNA levels ($P < 0.001$). Newman-Keul's test: * $P < 0.01$ as compared with 5 day-old rats; # $P < 0.01$ comparisons between jejunum and ileum; ^a $P < 0.01$ comparisons between enterocytes and crypts.

co-localizes with ApoER2 at the apical and endocytic vesicles, as the intercenter distances between the gold particles marking Dab2 and ApoER2 are < 80 nm (Fig. 8). Significant co-localization of Dab2/VLDLR is only observed in apical vesicles. Immunoreactive signal was not seen in the absence of the primary antibody (data not shown).

DISCUSSION

The intestinal endocytosis in mammals is highly active during the suckling period to absorb components of the mother's milk (see Fujita et al., 2007 for a review). Based on the effects of ontogeny and diet on the expression of Dab2 in rat small intestine, we proposed that Dab2 takes part in the intestinal endocytosis of milk macromolecules [Vázquez-Carretero et al., 2011]. The current results suggest the involvement of megalin/cubilin/amnionless/Dab2 multi-ligand receptor complex in the intestinal endocytosis during the suckling period mainly in the ileum. They also suggest that Dab2 participates in intestinal processes mediated by ApoER2 and VLDLR.

Immunocytochemical studies reveal for the first time that Dab2 co-localizes with either megalin, ApoER2 or VLDLR at the apical membrane and at the apical endocytic apparatus of the enterocytes, indicating that Dab2 may be an adaptor protein in processes mediated by these receptors at the apical domain of the intestinal epithelium.

Comparisons of the effects of intestinal region, age and diet on the expression of megalin, ApoER2 and VLDLR with those on Dab2 expression previously reported [Vázquez-Carretero et al., 2011] reveal that only the megalin expression profile resembles that of Dab2. Their mRNA and protein levels are: higher in the intestine of the suckling than in the adult, higher in the ileum than in the jejunum and up-regulated by components of the milk. This up-regulation is greater in the ileum than in the jejunum in the case of Dab2 and is only observed in the ileum for megalin. In addition, as observed with Dab2 [Vázquez-Carretero et al., 2011], during the suckling period the specific immunostaining of megalin is concentrated at the supranuclear region of the cytosol of the enterocytes. After weaning both, Dab2 [Vázquez-Carretero et al., 2011] and megalin (current observations) disappear from the supranuclear region and localize at the terminal web domain. The observed development-related effects on both, gene expression and intracellular location of Dab2 and megalin correlate with those reported for the apical endocytic apparatus of the enterocytes, which is assembled during the last 2–3 days of gestation and is greatly reduced at weaning, so that the intestinal permeability to milk macromolecules is terminated at day 21 after birth [Wilson et al., 1991; Fujita et al., 2007].

The results discussed so far support the view that megalin/Dab2 participate in the intestinal endocytosis of milk components, mainly in the ileum, but additional observations suggest that in the intestine of the suckling rat megalin/Dab2 may work in association with cubilin and amnionless. Thus, Dab2 [Vázquez-Carretero et al., 2011], megalin, cubilin, and amnionless (current results): (i) mRNAs levels are higher in the ileum than in the jejunum, (ii) present similar cellular location at the light microscope: are located in the cells lining the villus, but not in the crypts, mainly in the cytosolic supranuclear region of the enterocytes during the suckling period, but are not longer seen in that location after weaning, and (iii) co-localize at the apical endocytic apparatus of the epithelium, indicating their

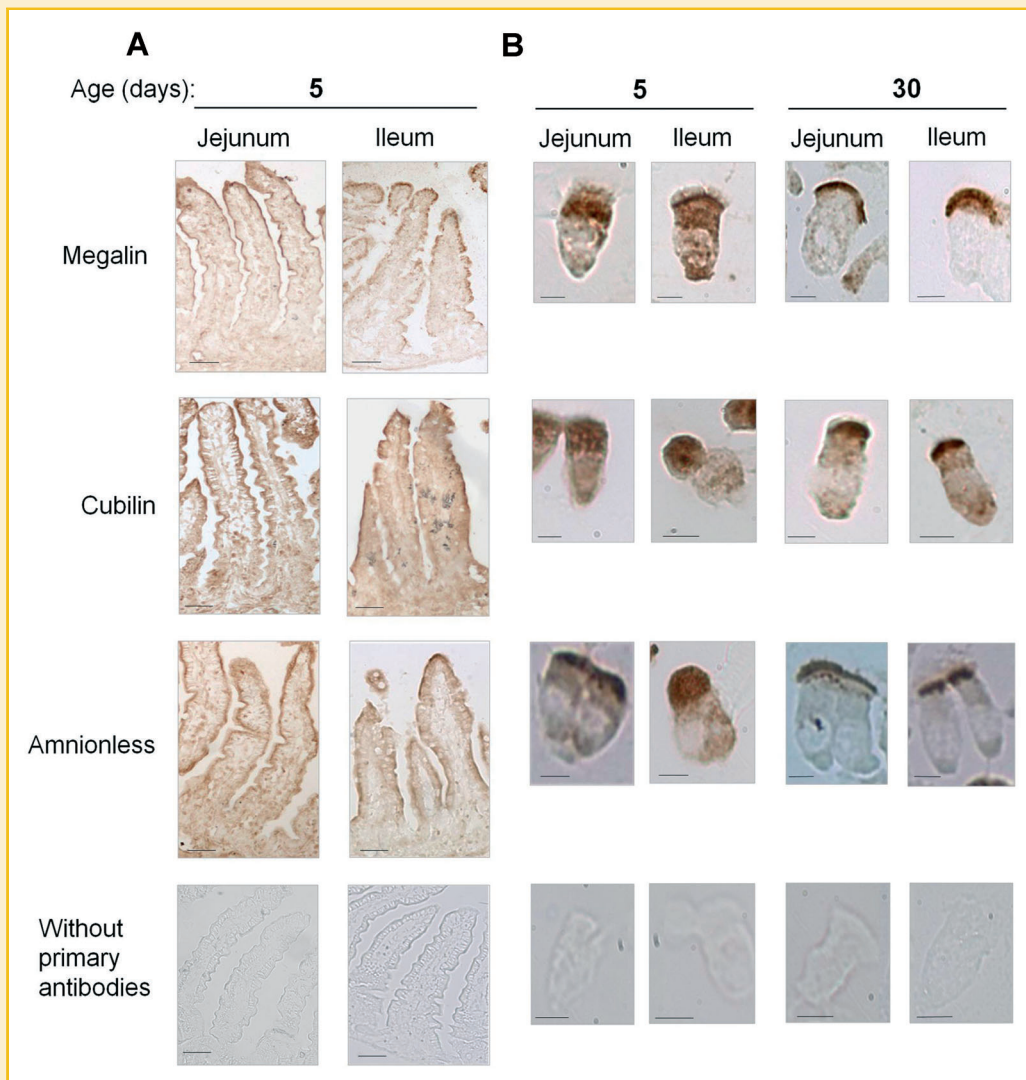


Fig. 5. Immunolocalization of megalin, cubilin and amnionless in rat small intestine. **A:** 10 μm cryosections of jejunum and ileum of 5 day-old rats. Scale bar represents 50 μm . **B:** Enterocytes isolated from jejunum and ileum of 5 and 30 day-old rats. Scale bar represents 5 μm . They were immunostained with either anti-megalin (Santa Cruz, dilution 1:25 in tissue sections and Acris, 1:100, in isolated cells), anti-cubilin (1:50) or anti-amnionless (1:25) antibody. Controls were carried out without primary antibodies. The photographs are representative of three different assays.

localization within the same population of endocytic cargos. Previously, megalin [Birn et al., 1997; Yammani et al., 2001], cubilin [Levine et al., 1984; Birn et al., 1997], amnionless [Strope et al., 2004] and Dab2 [Collaco et al., 2010; Vázquez-Carretero et al., 2011] had been only individually detected at the apical membrane of the ileum, though association of cubilin and megalin in rat small intestine has been suggested [Yammani et al., 2001] and is known that complexes of cubilin/amnionless [Seetharam et al., 1981; Aminoff et al., 1999; Tanner et al., 2003] mediate endocytosis of vitamin B12/intrinsic factor (IF) in the ileum. Therefore, to our knowledge, this is the first report showing co-localization of the four proteins at the apical domain and endocytic apparatus of the intestinal epithelium of the suckling rat. The observation that weaning affects the mRNA levels of the four proteins differently suggests that in the adult intestine the

megalin/cubilin/amnionless/Dab2 does not function as a multi-ligand complex.

The components of the milk endocytosed by the intestine via megalin/cubilin/amnionless/Dab2 are yet undefined. Most of the studies on the function of megalin, cubilin, and amnionless have been done in kidney and reveal a large number of ligands, including components of the milk [see Christensen et al., 2012, 2013 for reviews]. The ligands that bind to megalin in the intestine had not been investigated and the only intestinal function attributed to cubilin/amnionless is the endocytosis of vitamin B12/IF by the ileum [Seetharam et al., 1981; Aminoff et al., 1999; Tanner et al., 2003], although complexes of megalin/cubilin [Seetharam and Yammani, 2003] and of megalin/cubilin/amnionless [Dali-Youcef and Andrés, 2009] have been considered to mediate the endocytosis of

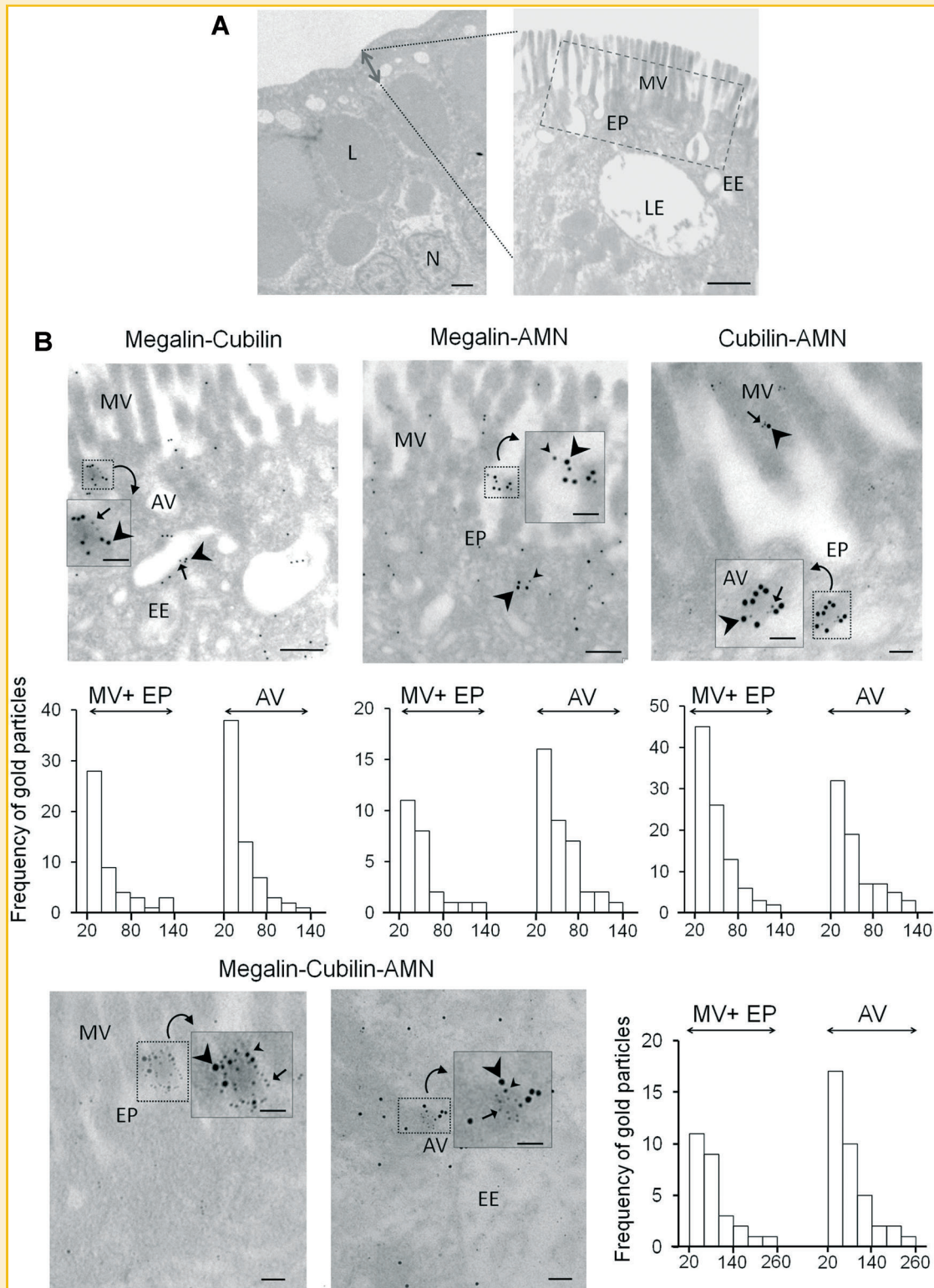


Fig. 6. Co-localization of megalin, cubilin and amnionless (AMN) in the epithelium of suckling rat ileum. 12–15 day-old rats were used. **A:** Electron microphotographs of the epithelial cells. Giant lysosome (L), nucleus (N), microvilli (MV), endocytic pits (EP), early endosomes (EE) and late endosomes (LE). The area within the square is that shown in B. Scale bar represents 1,000 nm. **B:** Immunogold analysis. The dilution of the antibodies was 1:20 for megalin (Acris) and 1:2 for cubilin and amnionless. Immunogold labeling of cubilin (6 nm) is indicated by arrows, that of megalin (10 nm) by small arrowheads and that of amnionless (15 nm) by large arrowheads. The photographs show staining at microvilli (MV), endocytic pits (EP) and apical vesicles (AV) of three different assays. Scale bar represents 100 nm and that in the insets, 50 nm. Histograms represent the frequency of gold particles distribution. Intercenter distances between gold particles were sorted into bins of 20 nm except for megalin/cubilin/amnionless that were 40 nm. The Chi-squared test ($P < 0.01$) showed significant co-localization for megalin/cubilin, megalin/AMN, cubilin/AMN and megalin/cubilin/AMN in all the studied compartments. For each cluster, the quantifications were done in 20–30 either microvilli, endocytic pits or apical vesicles.

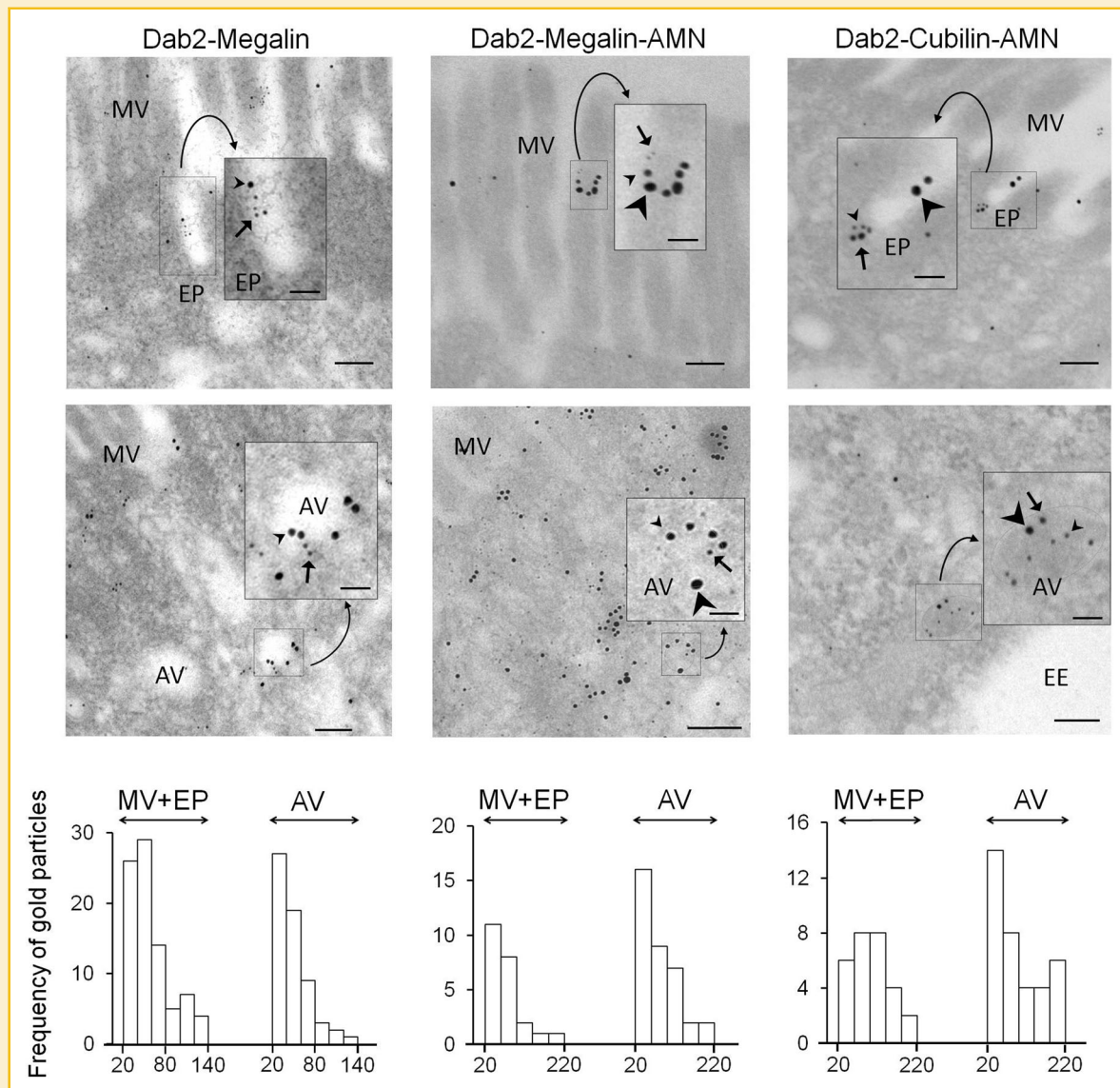


Fig. 7. Co-localization of megalin, cubilin, amnionless (AMN) and Dab2 in the epithelium of suckling rat ileum. 12–15 day-old rats were used. The dilution of the antibodies was 1:2 for Dab2, cubilin and amnionless and 1:20 for megalin (Acris). Immunogold labelling of cubilin (6 nm) is indicated by small arrowheads, that of megalin (10 nm) by small arrowheads, that of AMN (15 nm) by large arrowheads and that of Dab2 (6 and 10 nm) by arrows. In the histograms, intercenter distances between gold particles were sorted into bins of 20 nm for Dab2/megalín, 40 nm for Dab2/megalín/AMN and 40 nm for Dab2/cubilín/AMN. The Chi-squared test ($P < 0.01$) showed that gold labeling distribution is significantly different from random in all the studied compartments. See Figure 6 for other details.

vitamin B12/IF by the ileum. In addition, megalin/cubilín/amnionless exists as a complex that binds cobalamin/IF in renal membranes [Ahuja et al., 2008]. Therefore, a strong candidate to be endocytosed in the intestine by megalin/cubilín/amnionless/Dab2 could be the vitamin B12/IF complex, but some observations do not support this point of view. One is the low expression of IF in the suckling rats [Dieckgraefe et al., 1988]. Other is that megalin deficiency apparently does not result in defect intestinal cubilín endocytosis and cobalamin deficiency [see Christensen et al., 2012, 2013 for reviews]. However, Dali-Youcef and Andrés [2009] pointed out that about 1–5% of free cobalamin (or crystalline cobalamin) is absorbed along the entire intestine by passive diffusion and that this might explain the

mechanism underlying oral cobalamin treatment of cobalamin deficiencies. Further experiments are required to understand the role of megalin in the intestinal cobalamin-IF absorption. Folate-binding protein (FBP)-bound folate could be another candidate because its absorption is higher in the ileum than in the jejunum [Mason and Selhub, 1988] and megalin mediates the renal endocytosis of FBP [Birn et al., 2005]. Other components of the milk are the IgGs that are mainly absorbed in the jejunum by FcRn-mediated endocytosis [Fujita et al., 2007]. The unabsorbed IgGs are endocytosed in the ileum but the receptor for this remains unknown. Endocytosis of IgGs via megalin/cubilín complex has been reported in kidney proximal tubule [Birn et al., 2003] and in Opposum kidney

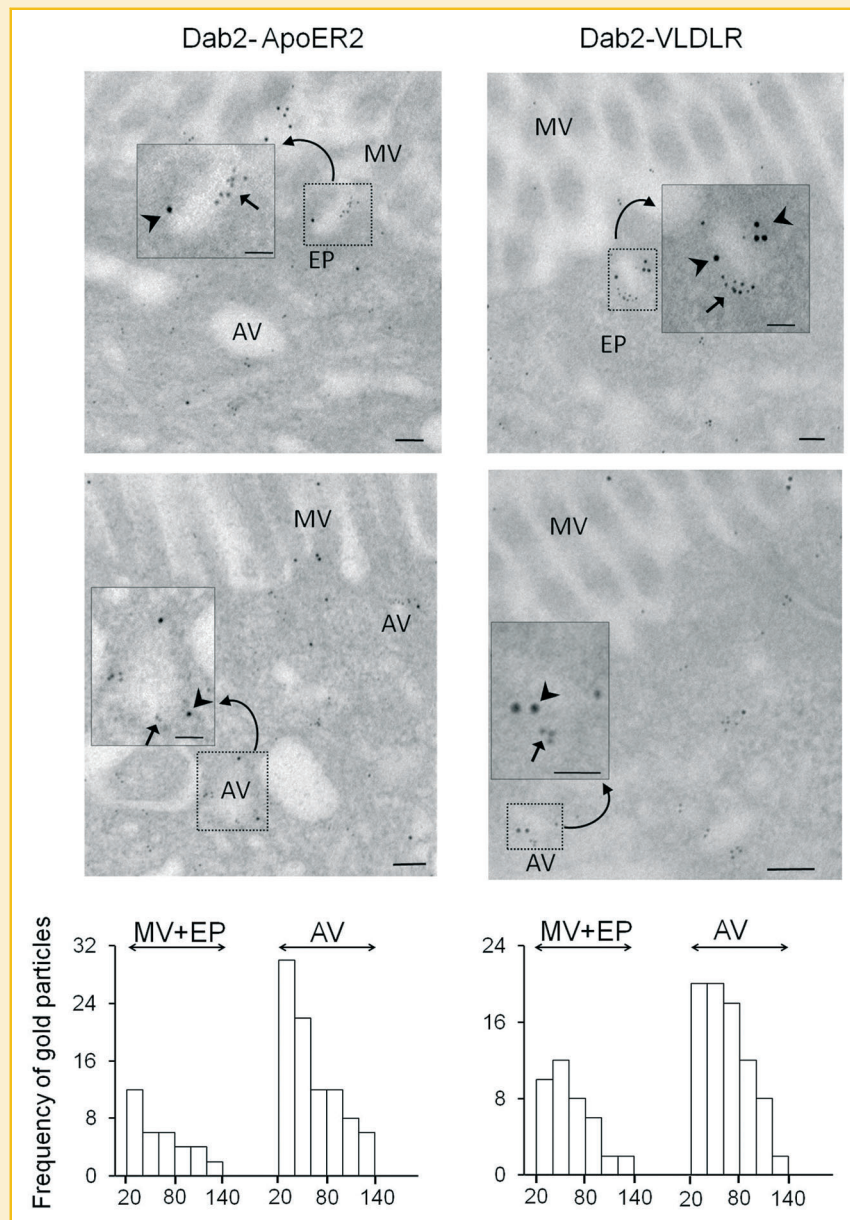


Fig. 8. Co-localization of VLDLR, ApoER2, and Dab2 in the epithelium of suckling rat ileum. 12–15 day-old rats were used. Dilution of antibodies was 1:15 for VLDLR, 1:300 for ApoER2 and 1:2 for Dab2. Immunogold labeling of Dab2 (6 nm) is indicated by arrows, that of VLDLR (10 nm) and that of ApoER2 (10 nm) by arrowheads. Scale bar represents 100 nm and that in the insets, 50 nm. In the histograms, intercenter distances between gold particles were sorted into bins of 20 nm. The Chi-squared test ($P < 0.01$) showed significant co-localization of Dab2/ApoER2 in all the studied compartments and of Dab2/VLDLR in apical vesicles. See Figure 6 for other details.

epithelial cells [Nagai et al., 2011]. Whether the intestinal endocytosis of the substrates mentioned above is mediated either by megalin/cubilin/amnionless/Dab2 or by different combinations of the receptors and Dab2 requires further investigation. In addition, megalin/cubilin/amnionless could be the receptor for many macromolecules present in the milk.

The nature of the milk components that up-regulates megalin and Dab2 expression also remains unknown. It is pertinent to mention that Vitamins A and D, which are components of the milk, increase megalin mRNA levels in renal culture cells [Liu et al., 1998].

Little is known on the functions of VLDLR and ApoER2 receptors in tissues other than brain. Their co-localization with Dab2 at the apical membrane domain and within the apical endocytic apparatus imply their involvement in intestinal endocytic processes. Apart from our work, nothing has been reported on ApoER2 in the intestine and the current results reveal that neither age nor diet significantly affected ApoER2 expression. Intestinal VLDLR-mediated processes seem to acquire relevance after weaning, because its expression in the enterocytes is up-regulated at weaning and if any, is down-regulated by milk diet. Levy et al. [2007] implicated VLDLR in the intestinal

secretion of cholesterol but localized the receptor at the enterocytes basolateral membrane. Nakamura et al. [2000] proposed that VLDLR regulates cell growth in developing tissues, such as fetal intestine and intestinal cancer cells.

In conclusion, this is the first report showing in the epithelium of rat small intestine: (i) the apical co-localization of megalin, cubilin, amnionless and Dab2, (ii) that megalin expression is regulated by ontogeny and by components of the milk and (iii) the co-localization of Dab2 with either ApoER2 or VLDLR. We propose that Dab2 acts as an adaptor protein in intestinal processes mediated by these receptors.

ACKNOWLEDGMENTS

Supported by a grant from Junta de Andalucía (CTS 5884) and a fellowship from Spanish MEC (AP2007-04201) to MD Vázquez-Carretero. Electronmicroscopy images were obtained in the CITIUS, Universidad de Sevilla. We thank R García-Navarro (Dpto. Biología Celular, Universidad de Sevilla) for technical support and Dr. I Morillón (Dpto. Microbiología, Universidad de Navarra) for technical advice.

REFERENCES

Ahuja R, Yammani R, Bauer JA, Kalra S, Seetharam S, Seetharam B. 2008. Interactions of cubilin with megalin and the product of the amnionless gene (AMN): Effect on its stability. *Biochem J* 410:301–308.

Amsellem S, Gburek J, Hamard G, Nielsen R, Willnow TE, Devuyst O, Nexo E, Verroust PJ, Christensen EI, Kozyraki R. 2010. Cubilin is essential for albumin reabsorption in the renal proximal tubule. *J Am Soc Nephrol* 21:1859–1867.

Aminoff M, Carter JE, Chadwick RB, Johnson C, Gräsbeck R, Abdelaal MA, Broch H, Jenner LB, Verroust PJ, Moestrup SK, de la Chapelle A, Krahe R. 1999. Mutations in CUBN, encoding the intrinsic factor-vitamin B12 receptor, cubilin, cause hereditary megaloblastic anaemia 1. *Nat Genet* 21:309–313.

Bergersen LH, Morland C, Ormel L, Rinholm JE, Larsson M, Wold JF, Røe AT, Stranna A, Santello M, Bouvier D, Ottersen OP, Volterra A, Gundersen V. 2012. Immunogold detection of L-glutamate and D-serine in small synaptic-like microvesicles in adult hippocampal astrocytes. *Cereb Cortex* 22:1690–1697.

Birn H, Leboulleux M, Moestrup SK, Ronco PM, Aucuturier P, Christensen EI. 2003. Megalin, cubilin and immunoglobulin light chains: receptor-mediated uptake of light chains in kidney proximal tubule. In: Touchard G, Aucuturier P, Hermine O, Ronco PM, editors. *Monoclonal gammopathies and the kidney*. The Netherlands: Kluwer Academic. pp 37–48.

Birn H, Verroust PJ, Nexo E, Hager H, Jacobsen C, Christensen EI, Moestrup SK. 1997. Characterization of an epithelial approximately 460-kDa protein that facilitates endocytosis of intrinsic factor-vitamin B12 and binds receptor-associated protein. *J Biol Chem* 272:26497–26504.

Birn H, Zhai X, Holm J, Hansen SI, Jacobsen C, Christensen EI, Moestrup SK. 2005. Megalin binds and mediates cellular internalization of folate binding protein. *FEBS J* 272:4423–4430.

Bradford MM. 1976. A rapid and sensitive method for the quantitation of microgram quantities of protein utilizing the principle of protein-dye binding. *Anal Biochem* 72:248–254.

Christensen EI, Birn H, Storm T, Weyer K, Nielsen R. 2012. Endocytic receptors in the renal proximal tubule. *Physiology* 27:223–236.

Christensen EI, Nielsen R, Birn H. 2013. From bowel to kidneys: The role of cubilin in physiology and disease. *Nephrol Dial Transplant* 28:274–281.

Christensen EI, Verroust PJ. 2002. Megalin and cubilin, role in proximal tubule function and during development. *Pediatr Nephrol* 17:993–999.

Cihil KM, Ellinger P, Fellows A, Stolz DB, Madden DR, Swiatecka-Urban A. 2012. Disabled-2 protein facilitates assembly polypeptide-2-independent

recruitment of cystic fibrosis transmembrane conductance regulator to endocytic vesicles in polarized human airway epithelial cells. *J Biol Chem* 287:15087–15099.

Collaco A, Jakab R, Hegan P, Mooseker M, Ameen N. 2010. Alpha-AP-2 directs myosin VI-dependent endocytosis of cystic fibrosis transmembrane conductance regulator chloride channels in the intestine. *J Biol Chem* 285:17177–17187.

Cuitino L, Matute R, Retamal C, Bu G, Inestrosa NC, Marzolo MP. 2005. ApoER2 is endocytosed by a clathrin-mediated process involving the adaptor protein Dab2 independent of its Rafts' association. *Traffic* 6:820–838.

Dali-Youcef N, André E. 2009. An update on cobalamin deficiency in adults. *QJM* 102:17–28.

Dieckgraefe BK, Seetharam B, Alpers DH. 1988. Developmental regulation of rat intrinsic factor mRNA. *Am J Physiol* 254:G912–G919.

Fujita M, Baba R, Shimamoto M, Sakuma Y, Fujimoto S. 2007. Molecular morphology of the digestive tract; macromolecules and food allergens are transferred intact across the intestinal absorptive cells during the neonatal-suckling period. *Med Mol Morphol* 40:1–7.

Fyfe JC, Madsen M, Højrup P, Christensen EI, Tanner SM, de la Chapelle A, He Q, Moestrup SK. 2004. The functional cobalamin (vitamin B12)-intrinsic factor receptor is a novel complex of cubilin and amnionless. *Blood* 103:1573–1579.

García-Miranda P, Peral MJ, Ilundain AA. 2010. Rat small intestine expresses the reelin-Disabled-1 signalling pathway. *Exp Physiol* 95:498–507.

Hammad SM, Barth JL, Knaak C, Argraves WS. 2000. Megalin acts in concert with cubilin to mediate endocytosis of high-density lipoproteins. *J Biol Chem* 275:12003–12008.

He Q, Madsen M, Kilkenney A, Gregory B, Christensen EI, Vorum H, Højrup P, Schäffer AA, Kirkness EF, Tanner SM, de la Chapelle A, Giger U, Moestrup SK, Fyfe JC. 2005. Amnionless function is required for cubilin brush-border expression and intrinsic factor-cobalamin (vitamin B12) absorption in vivo. *Blood* 106:1447–1453.

Hwang ES, Hirayama BA, Wright EM. 1991. Distribution of the SGLT1 Na⁺/glucose cotransporter and mRNA along the crypt-villus axis of rabbit small intestine. *Biochem Biophys Res Commun* 181:1208–1217.

Keita AV, Söderholm JD. 2010. The intestinal barrier and its regulation by neuroimmune factors. *Neurogastroenterol Motil* 22:718–733.

Knickelbein RG, Aronson PS, Dobbins JW. 1988. Membrane distribution of sodium-hydrogen and chloride-bicarbonate exchangers in crypt and villus cell membranes from rabbit ileum. *J Clin Invest* 82:2158–2163.

Levine JS, Allen RH, Alpers DH, Seetharam B. 1984. Immunocytochemical localization of the intrinsic factor-cobalamin receptor in dog-ileum: Distribution of intracellular receptor during cell maturation. *J Cell Biol* 98:1111–1118.

Levy E, Spahis S, Sinnott D, Peretti N, Maupas-Schwalm F, Delvin E, Lambert M, Lavoie MA. 2007. Intestinal cholesterol transport proteins: An update and beyond. *Curr Opin Lipidol* 18:310–318.

Liu W, Yu WR, Carling T, Juhlin C, Rastad J, Ridefelt P, Akerström G, Hellman P. 1998. Regulation of gp330/megalin expression by vitamins A and D. *Eur J Clin Invest* 28:100–107.

Livak KJ, Schmittgen TD. 2001. Analysis of relative gene expression data using real-time quantitative PCR and the 2^{-ΔC_t} Method. *Methods* 25:402–408.

Maldonado-Báez L, Wendland B. 2006. Endocytic adaptors: Recruiters, coordinators and regulators. *Trends Cell Biol* 16:505–513.

Mason JB, Selhub J. 1988. Folate-binding protein and the absorption of folic acid in the small intestine of the suckling rat. *Am J Clin Nutr* 48:620–625.

Matthews JB, Hassan I, Meng S, Archer SY, Hrnjez BJ, Hodin RA. 1998. Na⁺-K⁺-2Cl⁻ cotransporter gene expression and function during enterocyte differentiation. Modulation of Cl⁻ secretory capacity by butyrate. *J Clin Invest* 101:2072–2079.

Maurer ME, Cooper JA. 2005. Endocytosis of megalin by visceral endoderm cells requires the Dab2 adaptor protein. *J Cell Sci* 118:5345–5355.

- Mishra SK, Keyel PA, Hawryluk MJ, Agostinelli NR, Watkins SC, Traub LM. 2002. Disabled-2 exhibits the properties of a cargo-selective endocytic clathrin adaptor. *EMBO J* 21:4915–4926.
- Moestrup SK, Kozyraki R, Kristiansen M, Kaysen JH, Rasmussen HH, Brault D, Pontillon F, Goda FO, Christensen EI, Hammond TG, Verroust PJ. 1998. The intrinsic factor-vitamin B12 receptor and target of teratogenic antibodies is a megalin-binding peripheral membrane protein with homology to developmental proteins. *J Biol Chem* 273:5235–5242.
- Morris SM, Arden SD, Roberts RC, Kendrick-Jones J, Cooper JA, Luzio JP, Buss F. 2002a. Myosin VI binds to and localises with Dab2, potentially linking receptor-mediated endocytosis and the actin cytoskeleton. *Traffic* 3:331–341.
- Morris SM, Cooper JA. 2001. Disabled-2 colocalizes with the LDLR in clathrin-coated pits and interacts with AP-2. *Traffic* 2:111–123.
- Morris SM, Tallquist MD, Rock CO, Cooper JA. 2002b. Dual roles for the Dab2 adaptor protein in embryonic development and kidney transport. *EMBO J* 21:1555–1564.
- Nagai J, Christensen EI, Morris SM, Willnow TE, Cooper JA, Nielsen R. 2005. Mutually dependent localization of megalin and Dab2 in the renal proximal tubule. *Am J Physiol* 289:F569–F576.
- Nagai J, Sato K, Yumoto R, Takano M. 2011. Megalin/cubilin-mediated uptake of FITC-labeled IgG by OK kidney epithelial cells. *Drug Metab Pharmacokin* 26:474–485.
- Nakamura Y, Yamamoto M, Kumamaru E. 2000. Very low-density lipoprotein receptor in fetal intestine and gastric adenocarcinoma cells. *Arch Pathol Lab Med* 124:119–122.
- Oleinikov AV, Zhao J, Makker SP. 2000. Cytosolic adaptor protein Dab2 is an intracellular ligand of endocytic receptor gp600/megalin. *Biochem J* 347:613–622.
- Pedersen GA, Chakraborty S, Steinhäuser AL, Traub LM, Madsen M. 2010. AMN directs endocytosis of the intrinsic factor-vitamin B(12) receptor cubam by engaging ARH or Dab2. *Traffic* 11:706–720.
- Seetharam B, Alpers DH, Allen RH. 1981. Isolation and characterization of the ileal receptor for intrinsic factor-cobalamin. *J Biol Chem* 256:3785–3790.
- Seetharam B, Yammani RR. 2003. Cobalamin transport proteins and their cell-surface receptors. *Expert Rev Mol Med* 5:1–18.
- Strope S, Rivi R, Metzger T, Manova K, Lacy E. 2004. Mouse amnionless, which is required for primitive streak assembly, mediates cell-surface localization and endocytic function of cubilin on visceral endoderm and kidney proximal tubules. *Development* 131:4787–4795.
- Tanner SM, Aminoff M, Wright FA, Liyanarachchi S, Kuronen M, Saarinen A, Massika O, Mandel H, Broch H, de la Chapelle A. 2003. Amnionless, essential for mouse gastrulation, is mutated in recessive hereditary megaloblastic anemia. *Nat Genet* 33:426–429.
- Vázquez-Carretero MD, García-Miranda P, Calonge ML, Peral MJ, Ilundáin AA. 2011. Regulation of Dab2 expression in intestinal and renal epithelia by development. *J Cell Biochem* 112:354–361.
- Vázquez-Carretero MD, Palomo M, García-Miranda P, Carvajal AE, Sánchez-Aguayo I, Calonge ML, Peral MJ, Ilundáin AA. 2012. Dab2 and low density lipoprotein receptors (LDLR) in rat small intestine. *FEBS J* 279:127–128.
- Weiser MM. 1973. Intestinal epithelial cell surface membrane glycoprotein synthesis I. An indicator of cellular differentiation. *J Biol Chem* 248:2536–2541.
- Wilson JM, Whitney JA, Neutra MR. 1991. Biogenesis of the apical endosome-lysosome complex during differentiation of absorptive epithelial cells in rat ileum. *J Cell Sci* 100:133–143.
- Yammani RR, Seetharam S, Seetharam B. 2001. Cubilin and megalin expression and their interaction in the rat intestine: Effect of thyroidectomy. *Am J Physiol Endocrinol Metab* 28:900–907.
- Yang DH, Smith ER, Roland IH, Sheng Z, He J, Martin WD, Hamilton TC, Lambeth JD, Xu XX. 2002. Disabled-2 is essential for endodermal cell positioning and structure formation during mouse embryogenesis. *Dev Biol* 251:27–44.

SUPPORTING INFORMATION

Additional supporting information may be found in the online version of this article at the publisher's web-site.